

ESTIMATE OF ENHANCEMENTS IN SUB-BARRIER HEAVY-ION FUSION CROSS SECTIONS DUE TO COUPLING TO INELASTIC AND TRANSFER REACTION CHANNELS

R.A. BROGLIA

The Niels Bohr Institute, University of Copenhagen, Blegdamsvej 17, DK-2100 Copenhagen Ø, Denmark

C.H. DASSO, S. LANDOWNE

Nordita, Blegdamsvej 17, DK-2100 Copenhagen Ø, Denmark

and

G. POLLAROLO

*Istituto di Fisica Teorica dell'Università di Torino, Turin, Italy
and INFN Sezione di Torino, Turin, Italy*

Received 4 August 1983

Sub-barrier fusion cross sections for $^{40}\text{Ar} + ^{122}\text{Sn}$, $^{58}\text{Ni} + ^{58}\text{Ni}$ and $^{58}\text{Ni} + ^{64}\text{Ni}$ are estimated using a simplified model to account for couplings to inelastic excitation and transfer reaction channels. Couplings to inelastic modes generally account for the bulk of the sub-barrier cross sections. In the case of $^{58}\text{Ni} + ^{64}\text{Ni}$, positive Q -value transfer reaction channels are required to explain the trend of the low-energy fusion data.

It has been observed for a variety of heavy systems that low-energy fusion cross sections are much larger than can be explained from one-dimensional barrier penetration calculations [1–4]. The clear need to go beyond the conventional approach has stimulated several attempts to study the effects which additional degrees of freedom have on the low-energy fusion rates [1,5–10]. In the present contribution we apply the coupled channel formalism of refs. [8,9] to study the effects which inelastic excitation and transfer reaction processes have on the fusion of $^{40}\text{Ar} + ^{122}\text{Sn}$, $^{58}\text{Ni} + ^{58}\text{Ni}$ and $^{58}\text{Ni} + ^{64}\text{Ni}$.

A convenient framework to estimate the contribution of individual channels to the enhancement of sub-barrier fusion is provided by the two-level model of ref. [8]. The coupling matrix which controls the transmission flux through the barrier for a single excited state may be written as [9]

$$\langle n | H | n' \rangle = \langle n | -\tilde{Q}a^+a + F(a^+ + a) | n' \rangle, \quad (1)$$

where

$$a^+ | 0 \rangle = | 1 \rangle, \quad a | 0 \rangle = 0; \quad n = 0, 1. \quad (2)$$

In this expression F represents the strength of the coupling between the ground state and the excited state at the position r_b of the potential barrier. The quantity \tilde{Q} stands for the net gain of relative motion energy in the excited channel,

$$\tilde{Q} = Q + \Delta V_b \quad (3)$$

where Q is the reaction Q -value and ΔV_b is the change with respect to the entrance channel barrier height, $V_b = V(r_b)$ [7].

For an harmonic mode the condition $n \leq 1$ in eq. (2) amounts to a truncation of the set of intrinsic states, which is formally justified only in the weak coupling regime ($|F/\tilde{Q}| < 1$). However, in this case the matrix (1) leads to a fair estimate of the effects of the coupling on the transmission functions even in the strong coupling limit [9].

In order to make simple estimates of the combined effect of different reaction modes we consider the ine-

lastic and transfer channels to form a set of independent excitations. We thus make the straightforward generalization

$$H \rightarrow \sum_i H_i, \quad (4)$$

and diagonalize the coupling matrix in the corresponding product space. The transmission function is then given by [9]

$$T(E) = \sum_m |U_{m0}|^2 \{1 + \exp[(V_b + \lambda_m - E)/\epsilon]\}^{-1}, \quad (5)$$

where U_{m0} is the overlap of the ground state with the eigenvector of the coupling matrix corresponding to the eigenvalue λ_m and

$$\epsilon = \{-\hbar^2 [d^2 V(r_b)/dr^2]/\mu\}^{1/2}/2\pi \quad (6)$$

is a measure of the barrier thickness.

The transmission function should be calculated for each partial wave in order to construct the fusion cross section. However it is convenient to assume that the barrier position and its curvature are approximately the same for all partial waves. In this case the fusion cross section is simply given by [11]

$$\sigma_f(E) = \frac{\pi r_b^2 \epsilon}{E} \sum_m |U_{m0}|^2 \ln\{1 + \exp[(E - V_b - \lambda_m)/\epsilon]\}. \quad (7)$$

Eq. (7) shows that the cross section at energies well below the lowest effective barrier is enhanced with respect to the limit of no coupling by a factor

$$\mathcal{E} = \sum_m |U_{m0}|^2 \exp(-\lambda_m/\epsilon). \quad (8)$$

For a single mode, this reduces to [9]

$$\mathcal{E} \simeq F^2 \exp(-\lambda/\epsilon)/(F^2 + \lambda^2), \quad (9)$$

$$\lambda = [-\tilde{Q} - (\tilde{Q}^2 + 4F^2)^{1/2}]/2.$$

Table 2

Excitation energies E^* , deformation parameters β , coupling strengths F and enhancement factors \mathcal{E} for the inelastic channels included in the calculations.

| Nucleus | State (J) | E^* (MeV) | β | F (MeV) | \mathcal{E} |
|-------------------|------------------|-------------|---------|-----------|---------------|
| ^{40}Ar | 2^+ a) | 1.46 | 0.22 | -1.93 | 6.4 |
| | 3^- a) | 3.68 | 0.23 | -2.42 | 6.0 |
| | 4^+ a) | 2.89 | 0.11 | -1.23 | 1.9 |
| ^{122}Sn | 2^+ b) | 17.5 | 0.26 | -2.33 | 1.6 |
| | 2^+ c) | 1.14 | 0.12 | -1.41 | 3.4 |
| | 3^- c) | 2.49 | 0.15 | -2.26 | 7.0 |
| | 4^+ c) | 2.14 | 0.06 | -0.97 | 1.6 |
| | 5^- c) | 2.25 | 0.09 | -0.50 | 2.8 |
| ^{58}Ni | 2^+ b) | 12.1 | 0.16 | -1.88 | 1.6 |
| | 2^+ d) | 1.45 | 0.20 | -2.05 | 9.9 |
| | 3^- d) | 4.47 | 0.20 | -2.56 | 7.2 |
| ^{64}Ni | 4^+ d) | 2.46 | 0.12 | -1.63 | 3.6 |
| | 2^+ b) | 15.0 | 0.19 | -1.95 | 1.6 |
| | 2^+ e) | 1.34 | 0.19 | -1.92 | 8.4 |
| | 3^- e) | 3.60 | 0.15 | -1.89 | 3.8 |
| | 4^+ e) | 2.62 | 0.05 | -0.67 | 1.3 |
| | 2^+ b) | 15.0 | 0.19 | -1.92 | 1.5 |

a) Ref. [14]. b) Ref. [15]. c) Ref. [16]. d) Ref. [17]. e) Ref. [18].

This quantity is useful to judge the relative importance of different reaction channels in determining sub-barrier enhancements.

The coupling strengths for inelastic excitations may be estimated from the collective model expression

$$F_i^{(\text{in})} = (1/\sqrt{4\pi})[-\beta_i R dV_n(r_b)/dr + F_i^C(r_b)], \quad (10)$$

where $\beta_i R$ is the deformation length and V_n is the nuclear potential. The second term represents the usual form factor for Coulomb excitation. The factor $1/\sqrt{4\pi}$ results from averaging over all directions of the relative coordinate. In reactions with medium-heavy systems the one-particle form factors are roughly given by [12]

Table 1
Parameters for the nuclear potentials and resulting barriers.

| Nuclei (a + A) | V_0 (MeV) | R_{aA} (fm) | a_0 (fm) | V_b (MeV) | r_b (fm) | ϵ (MeV) |
|------------------------------------|-------------|---------------|------------|-------------|------------|------------------|
| $^{40}\text{Ar} + ^{122}\text{Sn}$ | -54.8 | 10.14 | 0.63 | 107.2 | 11.3 | 0.593 |
| $^{58}\text{Ni} + ^{58}\text{Ni}$ | -41.6 | 9.33 | 0.63 | 102.3 | 10.2 | 0.538 |
| $^{58}\text{Ni} + ^{64}\text{Ni}$ | -42.9 | 9.50 | 0.63 | 100.3 | 10.4 | 0.538 |

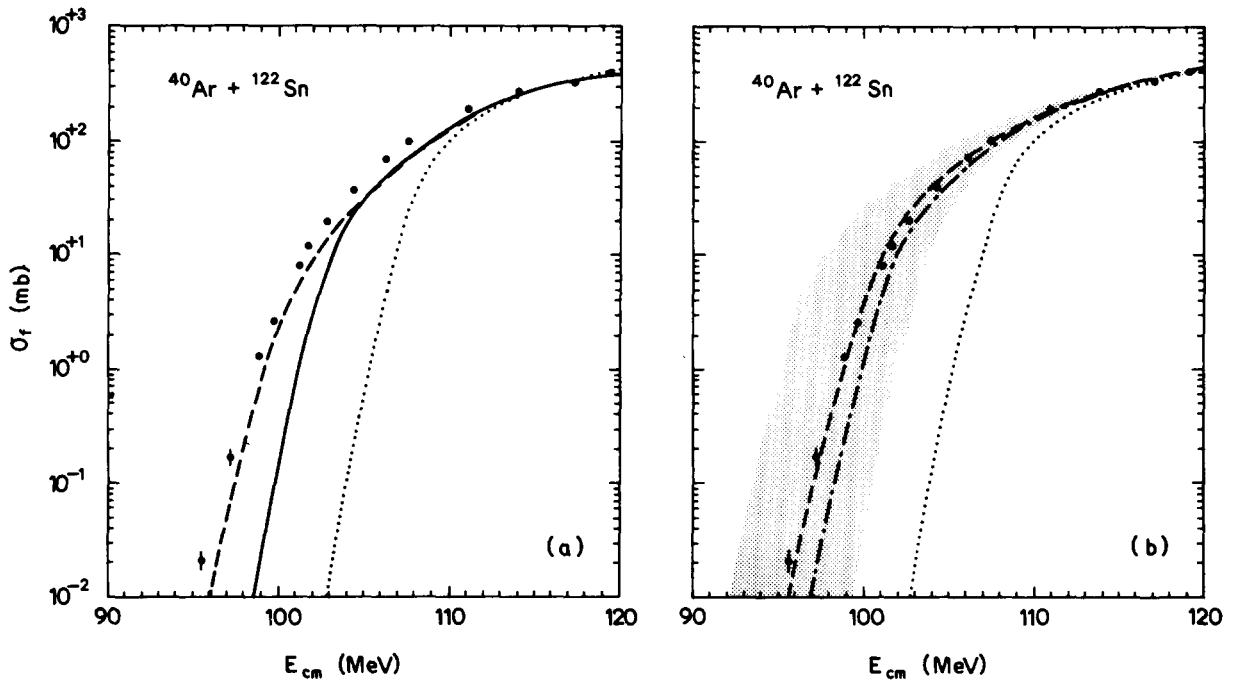


Fig. 1. Calculated fusion cross sections for $^{40}\text{Ar} + ^{122}\text{Sn}$. Part (a) shows the effect of coupling to the lowest 2^+ and 3^- states of the projectile and target compared to the limit of no-coupling (dotted curve) and the data of ref. [3]. The dashed curve results from setting the energies of the 2^+ and 3^- states to zero. In part (b) the dash-dotted curve results from including all of the inelastic channels of table 2. The dashed curve includes additional (1 MeV) strength at $\tilde{Q} = -15, -5$ MeV. The shaded area results from allowing 30% uncertainties in the coupling strengths.

$$F_i^{(\text{tr})} = (1/\sqrt{4\pi})(3 \text{ MeV}) \exp[-(r_b - R_1 - R_2)/a], \quad (11)$$

where $a = 1.2$ fm. Comparing eqs. (10) and (11) for typical parameters shows that the inelastic strength is about five times the transfer coupling. However, as the number of transfer channels is relatively large, they can not in general be ignored.

Using the above procedure, we have calculated fusion cross sections for the systems $^{40}\text{Ar} + ^{122}\text{Sn}$, $^{58}\text{Ni} + ^{58}\text{Ni}$ and $^{58}\text{Ni} + ^{64}\text{Ni}$. The nuclear potential parameters were determined by taking the Woods-Saxon formula of ref. [13] and then varying the strength of this potential to fit the fusion data above the barrier. This fixes the values of V_b , r_b and ϵ (table 1), which are similar to those obtained in other analyses [2,3]. For the inelastic modes we include the lowest states of various multiplicities and the giant quadrupole resonances of each nucleus. The coupling strengths were calculated from eq. (10) using deformation parameters deduced from the literature (table 2). The transfer

channels were accounted for in an average way, as discussed below.

In fig. 1a we show the results obtained for $^{40}\text{Ar} + ^{122}\text{Sn}$ when only the low-lying 2^+ and 3^- states are included (solid curve). These states were considered to account for the data in the zero-point fluctuation analysis of ref. [3]. However, this prescription neglects the excitation energies of the modes and overestimates the enhancement [9,10]. This can be seen from the dashed curve in fig. 1a which results from setting the energies of the 2^+ and 3^- states to zero.

The results in fig. 1a show that couplings to the low-lying 2^+ and 3^- states can not account for the observed sub-barrier cross section. By including all of the states in table 2 we obtain the dash-dotted curve shown in fig. 1b which still underpredicts the data. The giant quadrupole contributions to this calculation are relatively small and comparable to those of the low-lying 4^+ and 5^- states. To avoid diagonalizing a large matrix in this last calculation we used the follow-

ing approximation. The states whose enhancement factors are less than 3 (cf. table 2) were collected in ten-MeV energy bins centered at $\tilde{Q} = -15$ MeV and $\tilde{Q} = -5$ MeV. The corresponding coupling strength was taken to be the geometric average of the individual couplings. As all of the collective inelastic modes do not seem to give enough enhancement, we increased the coupling strength at $\tilde{Q} = -15$ MeV and $\tilde{Q} = -5$ MeV by 1 MeV in order to fit the data, as shown by the dashed curve in fig. 1b. The extra strength may be attributed to inelastic excitations and transfer reactions in these \tilde{Q} -value ranges.

Concerning the accuracy of these calculations we have checked that the approximation of taking a constant coupling works well for two channels coupled by a realistic nuclear form factor. Even though the $^{40}\text{Ar} + ^{122}\text{Sn}$ fusion data can be fairly well reproduced by the above procedure, it should be kept in mind that the form factors have uncertainties in their mag-

nitudes. The shaded area in fig. 1b is defined by allowing 30% variations in the coupling strengths. It is apparent from these results that in general it will be difficult to isolate effects which specific couplings may have on the sub-barrier fusion cross section.

Calculations for $^{58}\text{Ni} + ^{58}\text{Ni}$ are shown in fig. 2a. As in the case of $^{40}\text{Ar} + ^{122}\text{Sn}$, we have included couplings of 1 MeV at $\tilde{Q} = -15, -5$ MeV in addition to the inelastic modes of table 2. This gives the dashed curve which agrees reasonably well with the data. The shaded area again results from allowing 30% uncertainties in the coupling strengths.

The same procedure that is used to fit the $^{58}\text{Ni} + ^{58}\text{Ni}$ data results in the dash-dotted curve shown in fig. 2b when applied to the case of $^{58}\text{Ni} + ^{64}\text{Ni}$. As one would expect, this calculation has essentially the same low-energy behavior as for $^{58}\text{Ni} + ^{58}\text{Ni}$. Thus it fails to account for the relatively slower fall off of the $^{58}\text{Ni} + ^{64}\text{Ni}$ data. It was pointed out in ref. [7] that

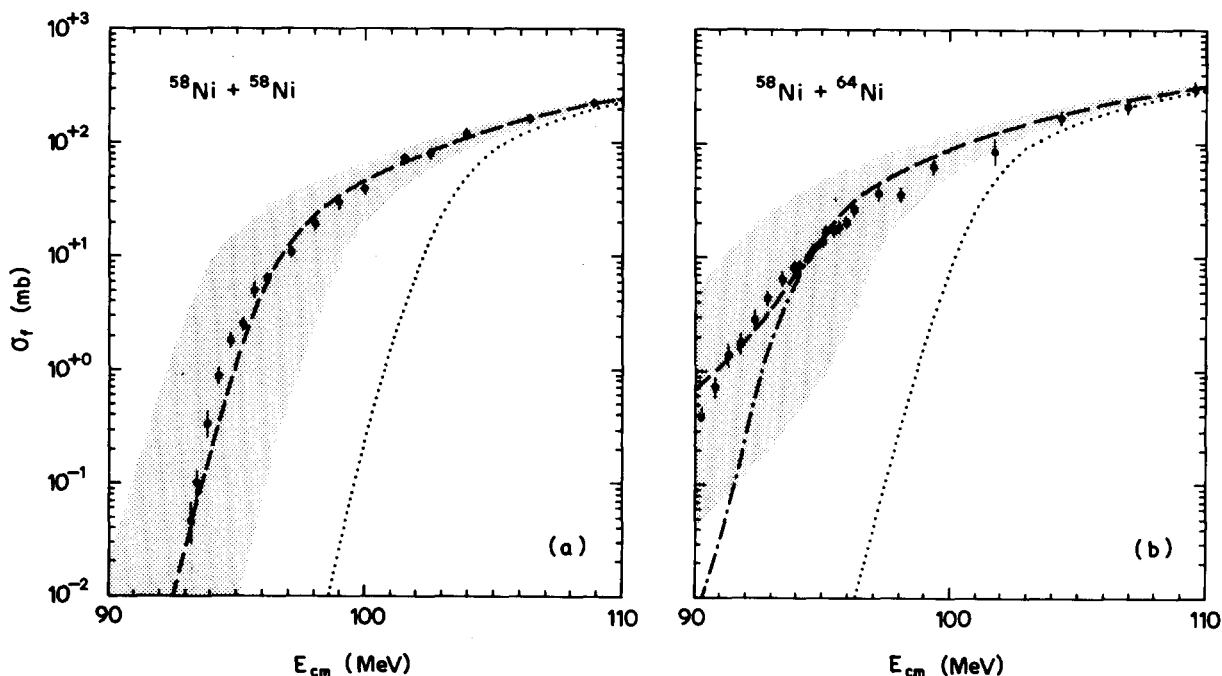


Fig. 2. Calculated fusion cross sections for (a) $^{58}\text{Ni} + ^{58}\text{Ni}$ and (b) $^{58}\text{Ni} + ^{64}\text{Ni}$ compared to the data of ref. [2]. The dotted curves show the limit of no-coupling. In part (a) the dashed curve includes all of the states in table 2 plus additional (1 MeV) strength at $\tilde{Q} = -15, -5$ MeV. The shaded area results from allowing 30% uncertainties in the coupling strengths. In part (b) the dash-dotted curve is obtained following the same prescription used to fit the $^{58}\text{Ni} + ^{58}\text{Ni}$ data in part (a). The dashed curve includes additional (1 MeV) strength at $\tilde{Q} = +5$ MeV, which must be attributed to transfer reaction channels. The shaded area results from allowing 30% uncertainties in the coupling strengths.

this feature is most likely due to the fact that the $^{58}\text{Ni} + ^{64}\text{Ni}$ combination allows for positive \tilde{Q} -value two-particle transfer reactions. Accordingly, we have added a coupling strength of 1 MeV at $\tilde{Q} = +5$ MeV in order to reproduce the trend of the data (dashed curve). We thus rely specifically on positive \tilde{Q} -value transfer reactions to change the slope of the low-energy cross section. This is apparent even when 30% uncertainties are introduced in the couplings, as shown by the shaded area.

Using the strength which seems to be required by the fusion data and the form of eq. (11) with $a = 0.6$ fm one can estimate the two-particle transfer reaction cross section which should be observed at positive Q -values. For instance, at $E = 100$ MeV we obtain a backward angle transfer cross section of about $10 \mu\text{b/sr}$.

References

- [1] R.G. Stokstad et al., Phys. Rev. Lett. 41 (1978) 465; Phys. Rev. C21 (1980) 2427; Z. Phys. A295 (1980) 269; R.G. Stokstad and E.E. Gross, Phys. Rev. C23 (1981) 281.
- [2] M. Beckerman et al., Phys. Rev. Lett. 45 (1980) 1472; Phys. Rev. C23 (1981) 1581; 25 (1982) 837; Phys. Rev. Lett. 50 (1983) 471.
- [3] W. Reisdorf et al., Phys. Rev. Lett. 49 (1982) 1811.
- [4] L.C. Vaz, J.M. Alexander and G.R. Satchler, Phys. Rep. 69 (1981) 373; U. Jahnke et al., Phys. Rev. Lett. 48 (1982) 17; W.S. Freeman et al., Phys. Rev. Lett. 50 (1983) 1563; R. Pengo et al., Contrib. Intern. Conf. on Heavy-ion physics and nuclear physics (Catania, 1983); Nucl. Phys. A, to be published.
- [5] H. Esbensen, Nucl. Phys. A352 (1981) 147.
- [6] S. Landowne and J.R. Nix, Nucl. Phys. A368 (1981) 352; B.V. Carlson and M.S. Hussein, Phys. Rev. C26 (1982) 2007; R. Lipperheide, H. Rossner and H. Massman, Nucl. Phys. A394 (1983) 312; M.J. Rhoades-Brown and V.E. Oberacker, Phys. Rev. Lett. 50 (1983) 1435.
- [7] R.A. Broglia, C.H. Dasso, S. Landowne and A. Winther, Phys. Rev. C27 (1983) 2433.
- [8] C.H. Dasso, S. Landowne and A. Winther, Nucl. Phys. A405 (1983) 381.
- [9] C.H. Dasso, S. Landowne and A. Winther, Nucl. Phys. A, to be published.
- [10] D.M. Brink, M.C. Nemes and D. Vauterin, Ann. Phys. to be published; P.M. Jacobs and U. Smilansky, Weizman Institute of Science preprint, WIS-13/83 March-Phy; M. Esbensen, Jian-Qun Wu and G.F. Bertsch, Michigan State University preprint (1983).
- [11] C.Y. Wong, Phys. Rev. Lett. 31 (1973) 766.
- [12] R.A. Broglia, G. Pollarolo and A. Winther, Nucl. Phys. A406 (1983) 369.
- [13] R.A. Broglia and A. Winther, Heavy ion reactions, Vol. 1 (Benjamin, Reading, MA, 1981) p. 114.
- [14] S. Sen and S.E. Darden, Nucl. Phys. A266 (1976) 173.
- [15] F.E. Bertrand, Nucl. Phys. A354 (1981) 129c.
- [16] O. Beer et al., Nucl. Phys. A147 (1970) 326.
- [17] A. Bernstein, Adv. Nucl. Phys. Vol. 3 (1969) 325.
- [18] G. Bruge et al., Nucl. Phys. A146 (1970) 597.